IDH2 inhibition enhances proteasome inhibitor responsiveness in hematological malignancies

Blood First Edition Paper, prepublished online November 19, 2018; DOI 10.1182/blood-2018-05-850826

IDH2 inhibition enhances proteasome inhibitor responsiveness in hematological malignancies

Elisa Bergaggio,[1] Chiara Riganti,[2] Giulia Garaffo,[1] Nicoletta Vitale,[1] Elisabetta Mereu,[1] Cecilia Bandini,[3-4] Elisa Pellegrino,[1] Verdiana Pullano,[1] Paola Omedè,[5] Katia Todoerti,[3-4] Luciano Cascione,[6] Valentina Audrito,[7] Anna Riccio,[8] Antonio Rossi,[9] Francesco Bertoni,[6] Silvia Deaglio,[7] Antonino Neri,[3-4] Antonio Palumbo,[1] and Roberto Piva[1]

[1]Department of Molecular Biotechnology and Health Sciences, University of Torino, Torino, Italy; [2]Department of Oncology, University of Torino, Torino, Italy; [3]Department of Oncology and Hemato-oncology, University of Milan, Milano, Italy; [4]Hematology Unit, Fondazione Cà Granda IRCCS, Ospedale Maggiore Policlinico, Milano, Italy; [5]Città Della Salute e della Scienza Hospital, Torino, Italy; [6]Università della Svizzera italiana, Institute of Oncology Research, Bellinzona, Switzerland; [7]Department of Medical Sciences, University of Torino; Italian Institute for Genomic Medicine, Torino, Italy; [8]Department of Biology, University of Rome Tor Vergata, Roma, Italy; and [9]Institute of Translational Pharmacology, Consiglio Nazionale delle Ricerche (CNR), Roma, Italy.

Correspondence: Roberto Piva, Department of Molecular Biotechnology and Health Sciences, University of Torino, via Nizza 52, Torino, 10126 Italy; e-mail: roberto.piva@unito.it; phone: +39-011-6334481; fax: +39-011-6335181.

Word counts for text and abstract: 3979 and 248.

Figure/table count: 6 figures.

Reference count: 58.

Key Points

- IDH2 is a new synthetic lethal target to proteasome inhibitors (PIs), efficacious in several hematological malignancies.
- Inhibition of NAMPT/SIRT3/IDH2 pathway could enhance the therapeutic efficacy and overcome resistance to PIs.

ABSTRACT

Proteasome inhibitors (PIs) are extensively used for the therapy of multiple myeloma (MM) and mantle-cell lymphoma (MCL). However, patients continuously relapse or are intrinsically resistant to this class of drugs. Here, to identify targets that synergize with PIs, we carried out a functional screening in MM cell lines using a short hairpin RNA library against cancer driver genes. *Isocitrate dehydrogenase 2* (*IDH2*) was identified as a top candidate, showing a synthetic lethal activity with the PI carfilzomib (CFZ). Combinations of FDA approved PIs with a pharmacological IDH2 inhibitor (AGI-6780) triggered synergistic cytotoxicity in MM, MCL, and Burkitt's lymphoma (BL) cell lines. CFZ/AGI-6780 treatment increased death of primary $CD138^+$ cells from MM patients and exhibited a favorable cytotoxicity profile towards peripheral blood mononuclear cells and bone marrow-derived stromal cells. Mechanistically, CFZ/AGI-6780 combination significantly decreased tricarboxylic acid (TCA) cycle activity and ATP levels, as a consequence of enhanced IDH2 enzymatic inhibition. Specifically, CFZ treatment reduced the expression of nicotinamide phosphoribosyltransferase (NAMPT), thus limiting IDH2 activation through the NAD^+-dependent deacetylase SIRT3. Consistently, combination of CFZ with either NAMPT or SIRT3 inhibitors impaired IDH2 activity and increased MM cell death. Finally, inducible IDH2 knockdown enhanced the therapeutic efficacy of CFZ in a subcutaneous xenograft model of MM, resulting in inhibition of tumor progression and extended survival. Taken together, these findings indicate that NAMPT/SIRT3/IDH2 pathway inhibition enhances the therapeutic efficacy of PIs, thus providing compelling evidence for treatments with lower and less toxic doses and broadening the application of PIs to other malignancies.

INTRODUCTION

The ubiquitin-proteasome pathway plays a crucial role in protein processing and degradation, regulating critical cellular functions including cell-cycle control, transcriptional regulation, cellular stress responses, and antigen presentation.[1] It is well established that proteasome inhibition results in the disruption of normal homeostatic mechanisms, and that malignant cells are more susceptible to the cytotoxic effects of proteasome inhibition than normal cells, most likely as a consequence of their increased requirement for protein synthesis and their higher levels of proteasome activity.[2] A number of processes have been reported to contribute to the antitumoral effects of proteasome inhibitors (PIs), including inhibition of the NF-κB pathway,[3] altered cell cycle control and apoptosis mechanisms,[4,5] endoplasmic reticulum stress, suppression of cell adhesion signaling, inhibition of angiogenesis and DNA repair.[2] The prevalent sensitivity of transformed cells to PIs and the successful design of clinical protocols, have led to the regulatory approval of PIs to treat multiple myeloma (MM) and mantle-cell lymphoma (MCL) patients.[6–10] To date, three PIs are routinely used in clinical settings (bortezomib, carfilzomib, and ixazomib), and additional PIs are under investigation.[11] The pleiotropic consequences of proteasome inhibition result in synergistic or additive activity with other therapeutic protocols including autologous stem cell transplantation (ASCT), glucocorticoids, alkylating agents and anthracyclines, immunomodulatory drugs, histone deacetylase inhibitors, and monoclonal antibodies.[10,12] Despite these enormous advances, relapses and disease progressions are common among MM patients, suggesting a prominent role for either innate or acquired drug-resistance.[13,14] Moreover, although the toxicity of PIs is quite well controlled in clinical settings, they display distinct adverse profiles, imposing limits to their doses.[15] In addition, responses to PIs in other hematological malignancies have been contradictory.[6,16,17] Similarly, promising preclinical data obtained with PIs in models of solid tumors have not been confirmed in the clinic,[15] probably as a consequence of impaired drug distribution, requiring higher dosages, not applicable for the toxic effects. Therefore, the design of a new generation of ubiquitin-proteasome pathway inhibitors and the identification of novel combination strategies is essential to overcome resistance and broaden the applicability of this class of drugs to other hematological malignancies, and possibly to solid tumors.

Here, to identify druggable targets which inhibition sensitize MM cells to PIs, we performed a short hairpin RNA functional screening targeting 152 cancer driver genes. Isocitrate

dehydrogenase 2 (IDH2) silencing revealed synthetic lethal activity with carfilzomib (CFZ). Combinations of the pharmacological IDH2 inhibitor AGI-6780 with PIs triggered synergistic cytotoxicity in MM, MCL, and Burkitt's lymphoma (BL) cell lines, as well as in primary $CD138^+$ cells from MM patients. Importantly, inducible IDH2 knock-down enhanced the therapeutic efficacy of CFZ in a subcutaneous xenograft model of MM. Our findings indicate that the NAMPT/SIRT3/IDH2 pathway is a major determinant of PIs responsiveness in hematological malignancies, thus providing proof of concept for new combination strategies to enhance sensitivity and overcome resistance to PIs.

MATERIALS AND METHODS

Detailed experimental procedures for cell culture conditions, shRNA screening, plasmid constructs, virus production, in vitro transduction, generation of inducible cell lines, purification of total RNA and Reverse Transcription-quantitative Polymerase Chain Reaction (RT-qPCR), DNA sequencing, western blotting, Gene Expression Profiling, analysis of apoptosis and cell cycle, analysis of reactive oxygen species (ROS) production, mitochondria isolation, and NF-κB activity are included in supplemental Material and Methods, available on the *Blood* web site.

Tricarboxylic acid (TCA) cycle measurement

The glucose flux through TCA cycle was measured by radiolabeling cells with 2 µCi/mL [6-^{14}C]-glucose (55 mCi/mmol; PerkinElmer, Waltham, Massachusetts, USA). Cell suspensions were incubated for 1 hour in a closed experimental system to trap the $^{14}CO_2$ developed from [^{14}C]-glucose, and the reaction was stopped by injecting 0.5 mL of 0.8 N $HClO_4$. The amount of glucose transformed into CO_2 through the TCA cycle was calculated as described,[18] and expressed as pmoles CO_2/h/mg cell proteins.

IDH enzymatic activity

Isocitrate Dehydrogenase Activity was measured using the IDH assay kit (Sigma-Aldrich, St. Louis, Missouri, USA), according to the manufacturer's protocol. IDH activity was determined using isocitrate as a substrate of the reaction, which results in a colorimetric (450 nm) product proportional to the enzymatic activity present. One unit of IDH is the amount of enzyme that generates 1.0 µmole of NADH or NADP per minute at pH 8.0 at 37°C. To evaluate IDH2 and IDH1 activities, mitochondrial or cytoplasmic extracts were respectively used.

Measurement of complex I–III activity

Mitochondria were extracted as described in supplemental Material and Methods. The electron flux from complex I to complex III was measured in 50 µL non-sonicated mitochondrial extracts, resuspended in 120 µL buffer A (5 mM KH_2PO_4, 5 mM $MgCl_2$, 5%

w/v BSA) in a 96 well plate. Then, 100 µL buffer B (25% w/v saponin, 50 mM KH_2PO_4, 5 mM $MgCl_2$, 5% w/v BSA, 0.12 mM cytochrome c-oxidized form, 0.2 mM NaN_3) was added for 5 min at room temperature. The reaction was started with 0.15 mM NADH and was followed for 6 min, reading the absorbance at 550 nm by a Lambda 3 spectrophotometer (PerkinElmer). Results were expressed as nmoles cytochrome c reduced/min/mg mitochondrial proteins.[19]

ATP measurement

The amount of ATP was measured in 50 µL mitochondrial extracts with the ATPlite assay (PerkinElmer), using a Synergy HT Multi-Mode Microplate Reader (Bio-Tek Instruments, Winooski, Vermont, USA). ATP was quantified as arbitrary light units; data were converted into nmoles/mg mitochondrial proteins, using a calibration curve previously set.

Xenograft models

KMS-27-TK-IDH2-A4 cells (5 x 10^5) suspended in phosphate-buffered saline (PBS)–50% Matrigel (BD Biosciences, San Jose, California, USA) were injected into the left and right flanks of NOD/SCID/IL2Rγ$^{-/-}$ (NSG) mice, previously anesthetized intramuscularly with xylazine and tiletamine/zolazepam. Tumor growth was monitored over time by determining the volume of tumor masses. Mice with tumor masses of 0.5 cm diameter (~3 weeks after the injection) were randomized and treated for 3 weeks with doxycycline by oral administration (0.1 mg/mL biweekly), CFZ i.v. (4 mg/kg biweekly), or the combination with the same dosing regimen used for the individual agents. Doxycycline was administrated in a 0.5% sucrose solution in light-proof bottles, for 48h. CFZ was dissolved in 3% DMSO, 10% Captisol (CYDEX Pharmaceuticals Inc., Lenexa Kansas, USA), 10 mM sodium citrate pH 3.5, and administrated after doxycycline removal. The control group received the carriers alone at the same schedule as the combination group. Mice were euthanized in a carbon dioxide chamber, after the tumor masses reached a volume of approximately 1 500 mm^3, or at early signs of distress. Tumor volume was calculated using the ellipsoid formula 4/3 x π x ½ x (length x width x depth). Animals were housed in the animal facility of the Molecular Biotechnology Center (Torino, Italy), in accordance with guidelines approved by the local Ethical Animal Committee. Experimental approval was obtained from the Italian Ministry of Health.

Statistical analysis

Statistical analyses were performed with GraphPad Prism 5.01 (GraphPad Software Inc.). Statistical significance of differences observed (in both in vitro and in vivo experiments) was determined by Student t test; differences were considered significant when *P* value was <.05 (*), <.01 (**), or <.001 (***). Survival curves were estimated with the Kaplan-Meier method. The log-rank test was used for statistical analysis.

RESULTS

shRNA screening in multiple myeloma cell lines identifies *IDH2* gene as synthetic lethal to the proteasome inhibitor carfilzomib

To identify druggable targets that synergize with PIs, we generated two MM cell lines (KMM-1^{PIR} and U266^{PIR}) cross-resistant to the PIs bortezomib (BTZ) and carfilzomib (CFZ) (supplemental Figure S1). A functional screening using a short hairpin RNA library targeting 152 cancer driver genes, highly representative of all signaling pathways, was carried out in the KMM-1^{PIR} cell line treated with sub-lethal concentrations of CFZ (Figure 1A-B; supplemental Table S1-6). The primary screening was validated in the U266^{PIR} cell line, by targeting the top 24 genes (supplemental Table S7). Analysis of the correlation between gene silencing efficacy and growth inhibition in presence of CFZ led to the identification of 3 synthetic lethal target genes (Figure 1C). Further studies were focused on isocitrate dehydrogenase 2 (IDH2), a $NADP^+$ dependent mitochondrial enzyme, that catalyzes the oxidative decarboxylation of isocitrate to α-ketoglutarate in tricarboxylic acid (TCA) cycle. To validate screening results, two shRNA sequences (A4 and A6) directed against human IDH2 were individually transduced into KMM-1^{PIR} and U266^{PIR} cells (supplemental Figure S2). IDH2 knockdown did not affect viability of KMM-1^{PIR} and U266^{PIR} cells. In contrast, IDH2 depletion was dramatically cytotoxic in cells treated with a sub-lethal dose of CFZ (Figure 1D-E). We excluded that *IDH2* mutations or its aberrant expression were associated to PIs resistance in MM cells (supplemental Figure S3). These findings prompted us to verify whether IDH2 knockdown could synergize with CFZ also in PI-sensitive cell lines. Accordingly, IDH2 silencing considerably enhanced sensitivity to CFZ in parental KMM-1 and U266 cell lines (Figure 1F-G). Taken together these data established that IDH2 knockdown is synthetic lethal to CFZ treatment in both PI resistant and sensitive MM cell lines.

Pharmacological inhibition of IDH2 enhances sensitivity to CFZ in MM cell lines

To define whether pharmacological inhibition of IDH2 recapitulates the synthetic lethal phenotype, CFZ treatment was associated to AGI-6780, an allosteric inhibitor of mutant IDH2, known to reduce the activity of wild type IDH2, although less potently.[20,21] We first demonstrated that AGI-6780 (5 μM) selectively impaired IDH2 enzymatic activity in MM

cells (supplemental Figure S4A-D). Next, the PIs resistant MM cell lines KMM-1^{PIR} and U266^{PIR} were treated with either CFZ, AGI-6780, or the combination of the two drugs. Combinatorial treatments significantly increased cell death, compared to single drugs (Figure 2A-B), confirming data obtained by IDH2 knockdown. This combination was effective also in MM cells resistant to very high concentrations of PIs (Figure 2C; supplemental Figure S5). To prove that the combined cytotoxicity of AGI-6780 and CFZ is not restricted to PI resistant cells, eight MM cell lines with different degrees of PI sensitivity were treated with a single dose of CFZ in combination or not with AGI-6780, refreshed every 48 hours. Enhanced sensitivity to the combination treatment in comparison with either agent alone was observed in all MM cell lines (Figure 2D; supplemental Figure S6A-B). In contrast, the chronic myelogenous leukemia cell line K-562 was unresponsive to both drugs and to their combination (Figure 2D). Increased sensitivity to CFZ was confirmed in two MM cell lines (KMS-27 and U266) by regimens with lower doses of CFZ administered every 48 hours in combination with AGI-6780 (supplemental Figure S6C-D). Considering that hypoxic bone marrow microenvironment favors MM progression and drug resistance, we tested if this environment could affect the response to PIs and AGI-6780.[22–24] We confirmed that the combination of the two drugs increased MM cell death, also in presence of cells cultured with 1% oxygen concentration (supplemental Figure S7). To elucidate mechanisms of synthetic lethality, cell cycle and apoptotic markers were analyzed. CFZ/AGI-6780 combination was associated with an increase of G0/G1 phase (supplemental Figure S8), down-modulation of cyclins, up-regulation of cyclin-dependent kinase inhibitors, proteolytic cleavage of the caspases substrate PARP-1, and activation of effector caspases 3, 7, and 9 (Figure 2E). To reduce the confounding effects of cell death induction, western blotting and cell cycle analysis were performed 24 hours post-treatment, when cells displayed comparable levels of viability (Figure 2F-G). To further define the molecular mechanisms involved and/or regulated by the synergistic activity of CFZ/AGI-6780, gene expression profiles were analyzed 6 and 12 hours after single or combination treatments, and compared with untreated control samples. Supervised analysis identified 115 genes differentially regulated by CFZ, while AGI-6780 treatment had negligible transcriptional effects. Remarkably, 261 genes were differentially expressed after combined treatment, and nearly all genes modulated by CFZ (106/115) were concordantly modified to a higher degree by CFZ/AGI-6780 treatment (supplemental Figure S9A). Pathway analyses confirmed that the classical targets of PIs such as unfolded protein response (UPR), NF-κB, cell cycle, and apoptosis, were affected in

response to CFZ alone and these effects were enhanced by the combination with AGI-6780 (supplemental Figure S9B). Collectively, these findings indicate that the CFZ/AGI-6780 regimen is effective against PI-resistant and PI-sensitive MM cells and elicits significant changes converging in cell cycle and apoptotic pathways.

IDH2 inhibition synergizes with first- and second-generation PIs in B-cell hematological malignancies

To expand the clinical relevance of our observations and demonstrate that IDH2 inhibition specifically synergize with PIs, we first demonstrated that MM cells treated with AGI-6780 displayed enhanced response to the FDA approved PIs bortezomib (BTZ) and ixazomib (IXA) (supplemental Figure S10A-B). Since PIs have been approved also for the treatment of MCL patients and their anticancer effects have been obtained in different types of hematological malignancies,[6,25] we tested whether IDH2 inhibition could synergize with PIs in B-cell non-Hodgkin lymphoma models. Remarkably, a dramatic increase of cell death was observed in all MCL and BL cell lines treated with CFZ/AGI-6780 combinations (Figure 3). We then asked whether increased IDH2 activity could impair the cytotoxicity of PIs. As it is known that SIRT3 protein de-acetylates IDH2 and enhances its activity under glucose deprivation,[26,27] we cultured KMM-1 cells in absence of glucose for 7 days and measured IDH1, IDH2, and IDH3 enzymatic activities. As expected, a stable induction of IDH2 activity was observed after glucose restriction (supplemental Figure S10C). Next, we evaluated whether IDH2 activation was able to rescue MM cells from the effect of CFZ/AGI-6780 combination. KMM-1 cells were conditioned by glucose deprivation for 24 hours and subsequently treated with CFZ, AGI-6780, or with the two agents. Significantly, glucose restriction increased the viability of CFZ- and CFZ/AGI-6780-treated cells, as compared to not starved cells (supplemental Figure S10D). Moreover, we performed a canonical rescue experiment overexpressing IDH2 and/or SIRT3 in KMM-1^{PIR} cells (supplemental Figure S10E). We observed that only the combined overexpression of the two genes was able to enhance IDH2 activity (supplemental Figure S10F). Concordantly, cells with hyperactivation of IDH2 treated with CFZ and AGI-6780 partially decrease cell death, compared to the cells with a basal IDH2 activity (supplemental Figure S10G). Taken together these results suggest that IDH2 activity antagonizes the therapeutic efficacy of first- and second-generation PIs and that pharmacological IDH2 inhibition is a suitable

strategy to enhance the therapeutic efficacy of PIs in MM and other B-cell hematological malignancies.

CFZ/AGI-6780 combinatorial treatment decreases TCA cycle activity and mitochondrial ATP production through the NAMPT/SIRT3/IDH2 pathway

To define the molecular mechanisms responsible for the synergy between PIs and IDH2 inhibition, we considered that targeting IDH2 activity could lead to a decrease of NADPH production, resulting in higher reactive oxygen species (ROS) levels.[28] Taking into account that oxidative stress has been identified as an important mechanism of PI cytotoxicity in myeloma and non-myeloma cells,[29,30] we hypothesized that CFZ/AGI-6780 combination could exacerbate ROS levels, thus leading to increased cell death. However, only a slight increase in mitochondrial ROS concentration was observed in MM cells treated with CFZ/AGI-6780 combination (supplemental Figure S11). Next, we evaluated if IDH2 inhibition could impair tricarboxylic acid (TCA) cycle activity.[28] Notably, we observed that CFZ/AGI-6780 combination more drastically decreased IDH2 and TCA cycle activities, despite CFZ treatment was ineffective (Figure 4A-D). In this setting, IDH2 inhibition was associated to a proportional increase in IDH1 and IDH3 activities (supplemental Figure S12). In addition, electron transport chain (ETC) flux and mitochondrial ATP synthesis were accordingly down-regulated in MM cells treated with the combination of the two drugs (Figure 4E-F). Subsequently, we examined the biochemical mechanisms whereby CFZ treatment could synergize with AGI-6780 to further decrease IDH2 activity. It is recognized that PIs inhibit NF-κB[10,31] and that expression of nicotinamide phosphoribosyltransferase (NAMPT), a rate-limiting enzyme in the NAD^+ synthesis and sirtuins activation,[32] is transcriptionally modulated by NF-κB.[33–35] Therefore, we reasoned that PIs could affect IDH2 activation through the NAMPT/NAD^+/SIRT3 pathway (Figure 5A). Consistent with this hypothesis, we demonstrated that CFZ treatment significantly reduced NF-κB activity in KMS-27 cells (Figure 5B). Accordingly, NAMPT expression levels were significantly down-regulated by CFZ treatment (Figure 5C). To confirm the involvement of the NAMPT/NAD^+/SIRT3 pathway, we associated CFZ with several NAMPT inhibitors (FK866, GMX-1778, and Nampt-IN-1). As expected, combination of CFZ with NAMPT inhibitors induced synergistic down-regulation of IDH2 and TCA activity (Figure 5D; supplemental Figure S13A), followed by MM cell death, confirming the synthetic lethality previously reported by Cagnetta, et al with BTZ and FK866 (Figure 5E; supplemental Figure S13B-

C).[36] Importantly, these results were phenocopied by associating CFZ treatment to SIRT3 inhibition, both using specific drugs (AGK7 and TYP-3) (Figure 5F-G; supplemental Figure S13D-E) and shRNAs targeting SIRT3 (supplemental Figure S13F-G).[37]

Taken together these data demonstrate that CFZ/AGI-6780 combination significantly decreases TCA cycle activity, as a consequence of enhanced IDH2 enzymatic inhibition. Specifically, CFZ treatment reduces NAMPT expression and thus limits IDH2 activation through the NAD^+-dependent deacetylase SIRT3.

Targeting IDH2 and proteasome activities triggers synergistic inhibition of human MM cells growth ex-vivo and in vivo with low toxicity to normal human cells

To evaluate whether IDH2 inhibition potentiates CFZ effect in primary cells from MM patients, buffy coats derived from bone marrow aspirates of 9 MM patients were cultured on a layer of HS-5, a bone marrow stromal cell line. Ex-vivo co-cultures were treated with CFZ/AGI-6780 combination or with the single drugs for 96 hours. Combination treatment significantly decreased viability of $CD138^+$ cells (Figure 6A). Next, we demonstrated that CFZ/AGI-6780 treatment exhibited a favorable cytotoxicity profile towards peripheral blood mononuclear cells and bone marrow-derived stromal cells, compared to KMS-27 (Figure 6B-C). Taking into account that AGI-6780 is not suitable for in vivo studies,[38] and that enasidenib (AG-221), the mutant IDH2 inhibitor used in the clinic, does not affect the activity of wild-type IDH2,[21] we exploited a conditional RNAi method to knock-down IDH2 expression.[39,40] To provide an in vivo proof of principle that IDH2 inhibition could increase the therapeutic efficacy of PIs in MM, we expressed an IDH2-shRNA (IDH2-A4) in KMS-27 cell line under the control of the doxycycline-regulated transcriptional repressor tTR-KRAB (TK). We next studied the growth patterns of KMS-27-TK-IDH2-A4 cells injected subcutaneously into the flanks of NOD/SCID/IL2Rγ$^{-/-}$ (NSG) mice. Mice with masses of 0.5 cm in diameter were treated with doxycycline (DOXY; 0.1 mg/mL biweekly), CFZ (4 mg/kg biweekly), or control diluents. Administration of either agent had a substantial effect on tumor growth, as compared to control mice (P<.0001). Importantly, when IDH2 silencing was combined to CFZ, there was a further significant reduction in tumor growth in relation to single treatments (CFZ vs CFZ/DOXY P=.0244; DOXY vs CFZ/DOXY P=.0238; Figure 6D). The median overall survival of mice treated with CFZ associated to IDH2 silencing was significantly longer than vehicle-treated mice (26 vs 49 days; P=.0001), or mice treated with either drug alone (35 days for CFZ and 38 days for DOXY) (Figure 6E).

Together, these findings indicate that the anti-tumor activity of CFZ/AGI-6780 combination extends to primary explants from MM patients with a favorable therapeutic index and provide an in vivo proof of principle that IDH2 inhibition could increase the therapeutic efficacy of PIs.

DISCUSSION

Even though PIs have led to substantial outcome improvements in MM and MCL patients, development of novel combination strategies is needed to overcome resistance and broaden the applicability of this class of drugs to other malignancies.

The present study identified IDH2 as a new synthetic lethal target to PIs, efficacious in several hematological malignancies including MM, MCL, and BL. We showed that the combined targeting of IDH2 and proteasome triggers synergistic inhibition of human MM ex-vivo and in vivo, with low toxicity to normal human cells. We demonstrated that the NAMPT/SIRT3/IDH2 pathway is a major determinant of PIs responsiveness, thus providing a proof of concept for new combination strategies to enhance sensitivity and broaden the application of PIs to other malignancies.

IDH2 is a mitochondrial enzyme that catalyzes the reversible oxidative decarboxylation of isocitrate to alpha-ketoglutarate, with concomitant reduction of $NADP^+$ to NADPH. Hotspot mutations in *IDH2* gene have been identified in acute myeloid leukemias (AML),[41,42] angioimmunoblastic T-cell lymphomas (AITL),[43] and several other malignancies.[42,44–47] *IDH2* mutations cause a loss of IDH2 activity and an enzymatic gain of function that catalyzes the conversion of alpha-ketoglutarate to (R)-hydroxyglutarate (2-HG), with consequences on metabolism, epigenetic state, and cellular differentiation.[48,49] The appreciation of the role of *IDH2* mutations in oncogenesis and their early occurrence prompted to the approval of the IDH2-mutant inhibitor enasidenib (AG-221) for the treatment of refractory/relapsed *IDH2*-mutated AML patients.

In contrast, the potential role of wild-type *IDH2* and its clinical relevance in cancers has been poorly investigated. It is thought that the impact of IDH2 expression on neoplastic progression and drug resistance differs with respect to the site of origin and histological type.[50–55] Our study suggests the hypothesis that inhibition of wild-type IDH2 may have therapeutic potentials, regardless of IDH2 expression levels. Concordantly, we excluded that the *IDH2* mutational status or its aberrant expression was associated to PIs responsiveness in MM cells. Analysis of gene expression profiling datasets did not detect significant changes of IDH2 expression in the evolution of MM disease (data not shown). However, evaluation of IDH2 enzymatic activity could be more appropriate to further dissect the relevance of IDH2 in tumor development and maintenance, as well as a possible prognostic factor.

We demonstrated that genetic and pharmacological inhibition of IDH2 synergizes with first- and second-generation PIs by enhancing tumor cells death. In contrast, induction of

IDH2 enzymatic activity through glucose starvation impairs the therapeutic efficacy of PIs, confirming that pharmacological IDH2 inhibition is a suitable strategy to enhance PIs effects.

Mechanistically, we observed that CFZ significantly down-regulates NAMPT expression levels, most likely through the inhibition of NF-κB.[33–35] NAMPT is a key NAD pathway intermediate that catalyzes the transfer of a phosphoribosyl group from 5-phosphoribosyl-1-pyrophosphate (PRPP) to nicotinamide, forming nicotinamide mononucleotide (NMN). It has been previously shown that NAMPT inhibition is synthetic lethal to BTZ in MM.[36] Here, we demonstrated that combination of CFZ with either NAMPT or SIRT3 inhibitors induces synergistic down-regulation of IDH2 activity through the impairment of NAMPT/SIRT3/IDH2 pathway. The strong impairment of this pathway drastically decreases IDH2 and TCA cycle activities, leading to ETC flux and mitochondrial ATP synthesis down-regulation. However, we could not exclude that additional mechanisms may contribute to the anti-tumoral effects of CFZ/AGI-6780 combination.

We showed that the combined targeting of IDH2 and proteasome activities triggers synergistic inhibition of primary human MM cells. Importantly, CFZ/AGI-6780 combination exhibits a favorable cytotoxicity profile toward peripheral blood mononuclear cells and bone marrow–derived stromal cells. Considering the efficacy of CFZ/AGI-6780 also in PI-resistant cell lines, we speculate that this combination could be successful also in relapsed and refractory MM patients. To answer this question, further studies in cohort of patients stratified for their PI response are required. We extended the clinical relevance of our observations proving that IDH2 inhibition synergizes with PIs in several B-cell non-Hodgkin lymphoma cell lines including MM, MCL, BL, and diffuse large B-cell lymphomas (data not shown). Our preclinical studies therefore provide the rationale for development of novel IDH2 inhibitors directed against wild type IDH2. These observations are in line with recent studies highlighting the importance of wild-type IDH1 as therapeutic potential.[56–58] A further interesting expansion to the present work would be to investigate whether IDH2 synthetic lethal interaction to PIs could also take place in cancer patients with mutant *IDH2*, such as AML, AITL, and other malignancies.

Finally, we provided an in vivo proof of principle that IDH2 inhibition enhances the therapeutic efficacy of CFZ in a subcutaneous xenograft model of MM, resulting in inhibition of tumor progression and extended survival. Owing to the lack of wt-IDH2 inhibitors suitable for an in vivo use, we exploited a conditional shRNA system to knock-down IDH2. In contrast to in vitro data, in vivo IDH2 inhibition has a more substantial effect

on tumor growth, probably as a consequence of higher gene silencing obtained with the inducible shRNA.

In conclusion, the present study identified IDH2 as a new synthetic lethal target to PIs, efficacious in several hematological malignancies. We demonstrated that the NAMPT/SIRT3/IDH2 pathway is a major determinant of PIs responsiveness, thus providing a proof of concept for new combination strategies to enhance sensitivity and broaden the application of PIs to other malignancies.

Acknowledgments

This work was supported by: Associazione Italiana per la Ricerca sul Cancro (AIRC), Milano, Italy; Fondazione CRT, Torino, Italy; University of Torino to R.P.; the Gelu Foundation to F.B.

Authorship

Contribution: E.B., carried out most of the experiments and contributed to the interpretation of biological data with G.G., E.M., E.P., N.V., C.B., V.P., S.D., and F.B.; G.G. and E.M. performed shRNA screening experiments and analysis; C.R. and V.A. performed biochemical studies; N.V. performed tumor xenograft studies; A. Ricci and A. Rossi developed PI resistant cell lines; K.T., L.C., and A.N. performed gene expression profiling experiments and bioinformatics analyses; P.O. and A.P. provided clinically annotated MM samples; R.P. designed the studies and supervised the project; R.P. and E.B. wrote the manuscript; all authors were involved in the final version of the manuscript.

Conflict-of-interest disclosure: The authors declare no competing financial interests.

Correspondence: Roberto Piva, Department of Molecular Biotechnology and Health Sciences, University of Torino, via Nizza 52, Torino, 10126 Italy; e-mail: roberto.piva@unito.it

REFERENCES

1. Glickman MH, Ciechanover A. The Ubiquitin-Proteasome Proteolytic Pathway: Destruction for the Sake of Construction. *Physiol. Rev.* 2002;82(2):373–428.
2. Crawford LJ, Walker B, Irvine AE. Proteasome inhibitors in cancer therapy. *J. Cell Commun. Signal.* 2011;5(2):101–10.
3. Hideshima T, Chauhan D, Schlossman R, Richardson P, Anderson KC. The role of tumor necrosis factor α in the pathophysiology of human multiple myeloma: therapeutic applications. *Oncogene*. 2001;20(33):4519–4527.
4. Schwartz, PhD, MD AL, Ciechanover, MD, PhD A. THE UBIQUITIN-PROTEASOME PATHWAY AND PATHOGENESIS OF HUMAN DISEASES. *Annu. Rev. Med.* 1999;50(1):57–74.
5. Li B, Dou QP. Bax degradation by the ubiquitin/proteasome-dependent pathway: involvement in tumor survival and progression. *Proc. Natl. Acad. Sci. U. S. A.* 2000;97(8):3850–5.
6. Manasanch EE, Orlowski RZ. Proteasome inhibitors in cancer therapy. *Nat. Rev. Clin. Oncol.* 2017;14(7):417–433.
7. National Cancer Institute (2016). SEER Cancer Statistics Review, 1975–2014, based on November 2016 SEER data submission, posted to the SEER web site, April 2017. Table 18.9, Myeloma, SEER relative survival (percent) by year of diagnosis, all races, males and females 2017. National Cancer Institute, Bethesda.
8. Pulte D, Redaniel MT, Brenner H, Jansen L, Jeffreys M. Recent improvement in survival of patients with multiple myeloma: variation by ethnicity. *Leuk. Lymphoma*. 2014;55(5):1083–1089.
9. Goy A, Bernstein SH, Kahl BS, et al. Bortezomib in patients with relapsed or refractory mantle cell lymphoma: updated time-to-event analyses of the multicenter phase 2 PINNACLE study. *Ann. Oncol.* 2008;20(3):520–525.
10. Gandolfi S, Laubach JP, Hideshima T, et al. The proteasome and proteasome inhibitors in multiple myeloma. *Cancer Metastasis Rev.* 2017;36(4):561–584.
11. Piva R, Ruggeri B, Williams M, et al. CEP-18770: A novel, orally active proteasome inhibitor with a tumor-selective pharmacologic profile competitive with bortezomib. *Blood*. 2008;111(5):2765–75.
12. Larsen JT, Kumar S. Evolving Paradigms in the Management of Multiple Myeloma: Novel Agents and Targeted Therapies. *Rare Cancers Ther.* 2015;3(1–2):47–68.
13. Chim CS, Kumar SK, Orlowski RZ, et al. Management of relapsed and refractory multiple myeloma: novel agents, antibodies, immunotherapies and beyond. *Leukemia*. 2018;32(2):252–262.
14. Palumbo A, Anderson K. Multiple Myeloma. *N. Engl. J. Med.* 2011;364(11):1046–1060.
15. Huang Z, Wu Y, Zhou X, et al. Efficacy of therapy with bortezomib in solid tumors: a review based on 32 clinical trials. *Futur. Oncol.* 2014;10(10):1795–1807.
16. Thimmulappa RK, Mai KH, Srisuma S, et al. Identification of Nrf2-regulated genes induced by the chemopreventive agent sulforaphane by oligonucleotide microarray. *Cancer Res.* 2002;62(18):5196–203.
17. Cloos J, Roeten MS, Franke NE, et al. (Immuno)proteasomes as therapeutic target in acute leukemia. *Cancer Metastasis Rev.* 2017;36(4):599–615.
18. Riganti C, Gazzano E, Polimeni M, et al. Diphenyleneiodonium Inhibits the Cell Redox Metabolism and Induces Oxidative Stress. *J. Biol. Chem.* 2004;279(46):47726–47731.
19. Wibom R, Hagenfeldt L, von Döbeln U. Measurement of ATP production and respiratory chain enzyme activities in mitochondria isolated from small muscle

biopsy samples. *Anal. Biochem.* 2002;311(2):139–51.
20. Wang F, Travins J, DeLaBarre B, et al. Targeted Inhibition of Mutant IDH2 in Leukemia Cells Induces Cellular Differentiation. *Science (80-.).* 2013;340(6132):.
21. Urban DJ, Martinez NJ, Davis MI, et al. Assessing inhibitors of mutant isocitrate dehydrogenase using a suite of pre-clinical discovery assays. *Sci. Rep.* 2017;7(1):12758.
22. Hu J, Handisides DR, Van Valckenborgh E, et al. Targeting the multiple myeloma hypoxic niche with TH-302, a hypoxia-activated prodrug. *Blood*. 2010;116(9):1524–7.
23. Colla S, Storti P, Donofrio G, et al. Low bone marrow oxygen tension and hypoxia-inducible factor-1α overexpression characterize patients with multiple myeloma: role on the transcriptional and proangiogenic profiles of CD138+ cells. *Leukemia*. 2010;24(11):1967–1970.
24. Das DS, Ray A, Das A, et al. A novel hypoxia-selective epigenetic agent RRx-001 triggers apoptosis and overcomes drug resistance in multiple myeloma cells. *Leukemia*. 2016;30(11):2187–2197.
25. Obrist F, Manic G, Kroemer G, Vitale I, Galluzzi L. Trial Watch: Proteasomal inhibitors for anticancer therapy. *Mol. Cell. Oncol.* 2015;2(2):e974463.
26. Someya S, Yu W, Hallows WC, et al. Sirt3 Mediates Reduction of Oxidative Damage and Prevention of Age-Related Hearing Loss under Caloric Restriction. *Cell*. 2010;143(5):802–812.
27. Yu W, Dittenhafer-Reed KE, Denu JM. SIRT3 protein deacetylates isocitrate dehydrogenase 2 (IDH2) and regulates mitochondrial redox status. *J. Biol. Chem.* 2012;287(17):14078–86.
28. Molenaar RJ, Maciejewski JP, Wilmink JW, van Noorden CJF. Wild-type and mutated IDH1/2 enzymes and therapy responses. *Oncogene*. 2018;1.
29. Maharjan S, Oku M, Tsuda M, Hoseki J, Sakai Y. Mitochondrial impairment triggers cytosolic oxidative stress and cell death following proteasome inhibition. *Sci. Rep.* 2014;4(1):5896.
30. Lipchick BC, Fink EE, Nikiforov MA. Oxidative stress and proteasome inhibitors in multiple myeloma. *Pharmacol. Res.* 2016;105:210–215.
31. Hideshima T, Richardson P, Chauhan D, et al. The proteasome inhibitor PS-341 inhibits growth, induces apoptosis, and overcomes drug resistance in human multiple myeloma cells. *Cancer Res.* 2001;61(7):3071–6.
32. Garten A, Schuster S, Penke M, et al. Physiological and pathophysiological roles of NAMPT and NAD metabolism. *Nat. Rev. Endocrinol.* 2015;11(9):535–546.
33. Audrito V, Serra S, Brusa D, et al. Extracellular nicotinamide phosphoribosyltransferase (NAMPT) promotes M2 macrophage polarization in chronic lymphocytic leukemia. *Blood*. 2015;125(1):111–23.
34. Audrito V, Managò A, La Vecchia S, et al. Nicotinamide Phosphoribosyltransferase (NAMPT) as a Therapeutic Target in BRAF-Mutated Metastatic Melanoma. *JNCI J. Natl. Cancer Inst.* 2018;110(3):.
35. Zhang LQ, Heruth DP, Ye SQ. Nicotinamide Phosphoribosyltransferase in Human Diseases. *J. Bioanal. Biomed.* 2011;3:13–25.
36. Cagnetta A, Cea M, Calimeri T, et al. Intracellular NAD^+ depletion enhances bortezomib-induced anti-myeloma activity. *Blood*. 2013;122(7):1243–55.
37. Outeiro TF, Kontopoulos E, Altmann SM, et al. Sirtuin 2 inhibitors rescue alpha-synuclein-mediated toxicity in models of Parkinson's disease. *Science*. 2007;317(5837):516–9.
38. Popovici-Muller J, Saunders JO, Salituro FG, et al. Discovery of the First Potent Inhibitors of Mutant IDH1 That Lower Tumor 2-HG *in Vivo*. *ACS Med. Chem. Lett.*

2012;3(10):850–855.
39. Piva R, Pellegrino E, Mattioli M, et al. Functional validation of the anaplastic lymphoma kinase signature identifies CEBPB and BCL2A1 as critical target genes. *J. Clin. Invest.* 2006;116(12):3171–82.
40. Piva R, Agnelli L, Pellegrino E, et al. Gene expression profiling uncovers molecular classifiers for the recognition of anaplastic large-cell lymphoma within peripheral T-cell neoplasms. *J. Clin. Oncol.* 2010;28(9):1583–90.
41. Figueroa ME, Abdel-Wahab O, Lu C, et al. Leukemic IDH1 and IDH2 Mutations Result in a Hypermethylation Phenotype, Disrupt TET2 Function, and Impair Hematopoietic Differentiation. *Cancer Cell*. 2010;18(6):553–567.
42. Molenaar RJ, Thota S, Nagata Y, et al. Clinical and biological implications of ancestral and non-ancestral IDH1 and IDH2 mutations in myeloid neoplasms. *Leukemia*. 2015;29(11):2134–2142.
43. Wang C, McKeithan TW, Gong Q, et al. IDH2R172 mutations define a unique subgroup of patients with angioimmunoblastic T-cell lymphoma. *Blood*. 2015;126(15):blood-2015-05-644591.
44. Yan H, Parsons DW, Jin G, et al. IDH1 and IDH2 mutations in gliomas. *N. Engl. J. Med.* 2009;360(8):765–73.
45. Pansuriya TC, van Eijk R, d'Adamo P, et al. Somatic mosaic IDH1 and IDH2 mutations are associated with enchondroma and spindle cell hemangioma in Ollier disease and Maffucci syndrome. *Nat. Genet.* 2011;43(12):1256–1261.
46. Amary MF, Bacsi K, Maggiani F, et al. IDH1 and IDH2 mutations are frequent events in central chondrosarcoma and central and periosteal chondromas but not in other mesenchymal tumours. *J. Pathol.* 2011;224(3):334–343.
47. Borger DR, Tanabe KK, Fan KC, et al. Frequent mutation of isocitrate dehydrogenase (IDH)1 and IDH2 in cholangiocarcinoma identified through broad-based tumor genotyping. *Oncologist*. 2012;17(1):72–9.
48. DiNardo CD, Jabbour E, Ravandi F, et al. IDH1 and IDH2 mutations in myelodysplastic syndromes and role in disease progression. *Leukemia*. 2016;30(4):980–4.
49. Yang H, Ye D, Guan K-L, Xiong Y. IDH1 and IDH2 mutations in tumorigenesis: mechanistic insights and clinical perspectives. *Clin. Cancer Res.* 2012;18(20):5562–71.
50. Chen X, Xu W, Wang C, et al. The clinical significance of isocitrate dehydrogenase 2 in esophageal squamous cell carcinoma. *Am. J. Cancer Res.* 2017;7(3):700–714.
51. Guirguis A, Elishaev E, Oh S-H, et al. Use of gene expression profiles to stage concurrent endometrioid tumors of the endometrium and ovary. *Gynecol. Oncol.* 2008;108(2):370–6.
52. Altenberg B, Greulich KO. Genes of glycolysis are ubiquitously overexpressed in 24 cancer classes. *Genomics*. 2004;84(6):1014–1020.
53. Wu D. Isocitrate dehydrogenase 2 inhibits gastric cancer cell invasion via matrix metalloproteinase 7. *Tumor Biol.* 2016;37(4):5225–5230.
54. Lv Q, Xing S, Li Z, et al. Altered expression levels of IDH2 are involved in the development of colon cancer. *Exp. Ther. Med.* 2012;4(5):801–806.
55. Tian G-Y, Zang S-F, Wang L, et al. Isocitrate Dehydrogenase 2 Suppresses the Invasion of Hepatocellular Carcinoma Cells via Matrix Metalloproteinase 9. *Cell. Physiol. Biochem.* 2015;37(6):2405–14.
56. Calvert AE, Chalastanis A, Wu Y, et al. Cancer-Associated IDH1 Promotes Growth and Resistance to Targeted Therapies in the Absence of Mutation. *Cell Rep.* 2017;19(9):1858–1873.
57. Wahl DR, Dresser J, Wilder-Romans K, et al. Glioblastoma Therapy Can Be

Augmented by Targeting IDH1-Mediated NADPH Biosynthesis. *Cancer Res.* 2017;77(4):960–970.

58. Zarei M, Lal S, Parker SJ, et al. Posttranscriptional Upregulation of IDH1 by HuR Establishes a Powerful Survival Phenotype in Pancreatic Cancer Cells. *Cancer Res.* 2017;77(16):4460–4471.

FIGURE LEGENDS

Figure 1. shRNA screening in multiple myeloma cell lines identifies *IDH2* gene as synthetic lethal to the proteasome inhibitor carfilzomib. (A) Experimental design of the shRNA screen to identify genes conferring sensitivity to carfilzomib (CFZ) in multiple myeloma cells. KMM-1^{PIR} cells were infected with 684 shRNAs targeting 152 cancer driver genes (day -3) and incubated in presence or absence of puromycin (day -2). KMM-1^{PIR} cells were then splitted and treated with 2.5 nM CFZ or with control diluent (DMSO) (day 0). Growth rate was calculated at day 3 and 7 post-treatment (supplemental Table S5), and positive hits selected according to the Z-score. Top 24 selected genes were validated in a secondary screening performed in U266^{PIR} cells. **(B)** Representation of the Z-score (y-axis) for every shRNA (x-axis) calculated on growth rate reduction for each shRNA. Red box highlights candidates with Z-score below -0.8 (day 7) (supplemental Table S6). **(C)** Correlation between percentage of gene silencing and percentage of growth inhibition in presence of CFZ for top 3 candidate genes (*IDH2*, *KDM1A*, and *SOX2*) in U266 ^{PIR} cells. **(D)** KMM-1^{PIR}, **(E)** U266^{PIR}, **(F)** KMM-1, and **(G)** U266 cell lines were transduced with the empty vector or shRNAs targeting IDH2 (shIDH2_A4, shIDH2_A6) and treated with CFZ (KMM-1^{PIR} and U266^{PIR}: 5 nM; KMM-1 and U266: 2.5 nM) or DMSO every 48h. Cell viability was measured by TMRM staining-flow cytometry 96 hours post-treatment (hpt) for KMM-1^{PIR} and U266^{PIR}, 48 hours post-treatment (hpt) for KMM-1 and U266. Data are the means ± s.d. of three independent experiments (**P*<.05; ***P*<.01).

Figure 2. Pharmacological inhibition of IDH2 enhances sensitivity to CFZ in MM cell lines. (A) KMM-1^{PIR} and **(B)** U266^{PIR} cells were treated with 2.5 nM CFZ in combination or not with 10 µM AGI-6780. Cell viability was measured by TMRM staining-flow cytometry 96 hours post-treatment. Data are the means ± s.d. of four independent experiments. **(C)** U266^{PIR50} cells were treated with 75 nM CFZ in combination or not with 10 µM AGI-6780. Cell viability was measured by TMRM staining-flow cytometry 72 hours post-treatment. Data are the means ± s.d. of four independent experiments. **(D)** Eight MM cell lines and the K-562 cell line were treated with CFZ (1.67 nM CFZ for KMS-18; 2.5 nM for RPMI-8226, KMS-27, SK-MM-1, and CMA-03; 5 nM for KMM-1, U266, and NCI-H929 cell lines) in combination or not with 5 µM AGI-6780 (2.5 µM for RPMI-8226). Treatment was performed every 48h for AGI-6780, only at day 0 for CFZ. Cell viability was measured by TMRM staining-flow cytometry 8 days post-treatment. Data are the means ± s.d. of three independent experiments (**P*<.05; ***P*<.01; ****P*<.001; #*P*≥.05). **(E)** Western blot of KMM-1 and NCI-H929 cells, untreated (UT), treated with DMSO, AGI-6780 (KMM-1: 5 µM; NCI-H929: 10 µM), CFZ (KMM-1: 5 nM; NCI-H929: 2.5 nM), or the combination of the two drugs. Cell lysates were immunoblotted using the indicated antibodies 24 hours post-treatment. Vinculin protein expression was included for protein loading normalization. **(F-G)** Cell viability of the experiment described above was measured by TMRM staining-flow cytometry 24 and 72 hours post-treatment (hpt), respectively.

Figure 3. IDH2 inhibition increases sensitivity to CFZ in mantle cell lymphoma and Burkitt's lymphoma cells. (A) JeKo-1, **(B)** SP-49, **(C)** Mino, **(D)** Granta-519, **(E)** HS-Sultan, and **(F)** Raji cells were left untreated (UT), treated with DMSO, CFZ, AGI-6780, or the combination of the two drugs. JeKo-1 cells were treated at time 0, 48h, and 96h with both drugs. SP-49 cells were treated at time 0 and 48h with both drugs and at 96h with AGI-6780. Mino cells were treated with both drugs at time 0 and with AGI-6780 at 48h and 96h. Granta-519 cells were treated at time 0h and 48h with both drugs and every 48h with AGI-6780. HS-Sultan cells were treated at time 0 with both drugs and every 48h with AGI-6780. Raji cells were treated at time 0 and 48h with both drugs and every 48h with AGI-

6780. Cell viability was measured by TMRM staining-flow cytometry at the indicated time points. Data are the means ± s.d. of four independent experiments (*P<.05; **P<.01; ***P<.001).

Figure 4. Combinatorial treatment with CFZ and AGI-6780 causes a reduction in IDH2 activity and mATP levels. (A) KMS-27 and **(B)** KMM-1^{PIR} cells untreated (UT), treated with DMSO, CFZ (2.5 nM and 5 nM, respectively), AGI-6780 (5 µM), or the combination of the two drugs were analyzed for IDH2 activity 6 hours post-treatment. **(C)** KMS-27 and **(D)** KMM-1^{PIR} cells treated as described above were analyzed for tricarboxylic acid (TCA) cycle activity 6 hours post-treatment. Data are the means ± s.d. of four independent experiments. **(E)** KMS-27 cells treated as described above were analyzed for electron transport chain (ETC) complexes I to III 7 hours post-treatment. **(F)** KMS-27 cells treated as described above were analyzed for mitochondrial ATP (mATP) production 7 hours post-treatment. Data are the means ± s.d. of three independent experiments (*P<.05; **P<.01; ***P<.001).

Figure 5. Combinatorial treatment with CFZ and AGI-6780 acts through the inhibition of the NAMPT/SIRT/IDH2 pathway. **(A)** Schematic representation of the NAMPT/SIRT3/IDH2 pathway and inhibitors. **(B)** KMS-27 cells treated with DMSO, AGI-6780 (5 µM), CFZ (3 nM), or the combination of the two drugs were analyzed for NF-κB activity 6 hours post-treatment. NF-κB activity was detected in total extracts measuring the DNA-binding capability of NF-κB on its target sequence (see Methods). Data represent the percentage of NF-κB binding activity normalized versus DMSO samples and are the means ± s.d. of three independent experiments. **(C)** KMS-27 cells untreated (UT), treated with DMSO, CFZ (2.5 nM), AGI-6780 (5 µM), or the combination of the two drugs were analyzed for NAMPT mRNA expression levels 24 hours post-treatment. Data are the means ± s.d. of three independent experiments. **(D-E)** KMS-27 cells were left untreated (UT), treated with DMSO or FK866 (10 nM), for 48 hours, vehicle or CFZ (2.5 nM) were added for additional 48 hours. Cells were analyzed for (D) IDH2 activity 6 hours post-treatment with CFZ and for (E) cell viability by TMRM staining-flow cytometry 6 and 48 hours post-treatment with CFZ (hpt). Data are the means ± s.d. of three independent experiments. **(F-G)** KMS-27 cells untreated (UT), treated with DMSO, 1.25 nM CFZ, 10 µM AGK7, or the combination of the two drugs were analyzed for (F) IDH2 activity 6 hours post-treatment and for (G) cell viability measured by TMRM staining-flow cytometry 6 and 48 hours post-treatment (hpt). Data are the means ± s.d. of three independent experiments (*P<.05; **P<.01; ***P<.001).

Figure 6. Targeting IDH2 and proteasome activities triggers synergistic inhibition of human MM cells growth ex-vivo and in vivo with low toxicity to normal human cells. (A) Buffy coats derived from bone marrow aspirates of MM patients were treated with CFZ (2.5 nM) in combination or not with AGI-6780 (5 µM). Cell viability was estimated by FACS measuring Annexin V$^-$ and CD138$^+$ cells 96 hours post-treatment. Histograms represent the percentage of viable cells normalized versus DMSO samples. Data are the means ± s.e.m. of nine independent MM patients. **(B)** Peripheral blood mononuclear cells (PBMCs) and KMS-27 were treated with DMSO, CFZ (1.25, 2.5, 5, 10 nM), AGI-6780 (5 µM), or the combination of the two drugs. PBMCs were derived from 4 healthy donors. Cell viability was measured by TMRM staining-flow cytometry 48h post-treatment. Data are the means ± s.d. (*P<.05; **P<.01; ***P<.001). **(C)** KMS-27-TK cells (expressing DsRed fluorescent protein) were co-coltured with HS-5 bone marrow/stroma cell line and treated with CFZ, AGI-6780, or the combination. Percentage of live DsRed$^+$ cells was measured overtime. Data are the means ± s.d. of three independent experiments (CFZ vs CFZ+AGI-6780

P<.01). **(D) Growth patterns of KMS-27-TK-IDH2-A4 cells injected subcutaneously into the flanks of NOD/SCID/IL2Rγ$^{-/-}$ (NSG) mice. Tumor masses of 0.5 cm diameter mice were randomized for treatment with vehicle (n = 6), 4 mg/kg CFZ (n = 8), 0.1 mg/mL DOXY (n = 10), or the combination of both compounds (n = 10) over 3 weeks. Administration of either agent had a substantial effect on tumor growth, as compared to control mice (P<.0001). Combination of IDH2 silencing with CFZ further reduced tumor growth in relation to single treatments (CFZ vs CFZ/DOXY P=.0244; DOXY vs CFZ/DOXY P=.0238). Each data point represents the average tumor volume (mean ± standard error of the mean) for the indicated treatment condition. The timeline shows the schedule of treatment followed for in vivo treatments. **(E)** Kaplan–Meier survival plot showing survival for mice treated with vehicle (n = 6), 4 mg/kg CFZ (n = 6), 0.1 mg/mL DOXY (n = 8), or their combination (n = 6). CFZ plus DOXY-treated mice show significantly increased survival (49 days) in comparison with vehicle-treated mice (26 days; P<.0001), CFZ alone (35 days; P=.0007), and DOXY alone (38 days; P=.0472).

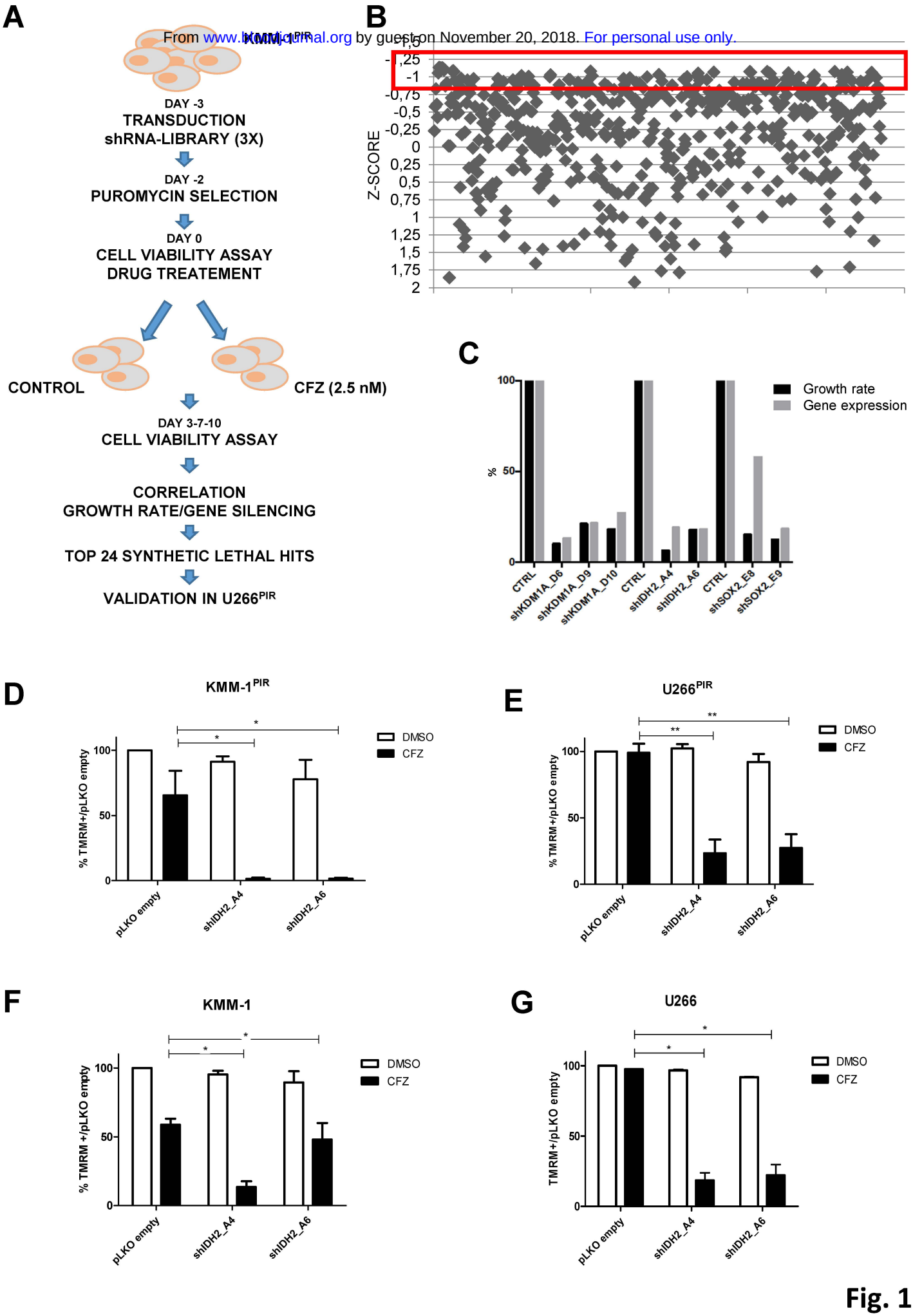

Fig. 1

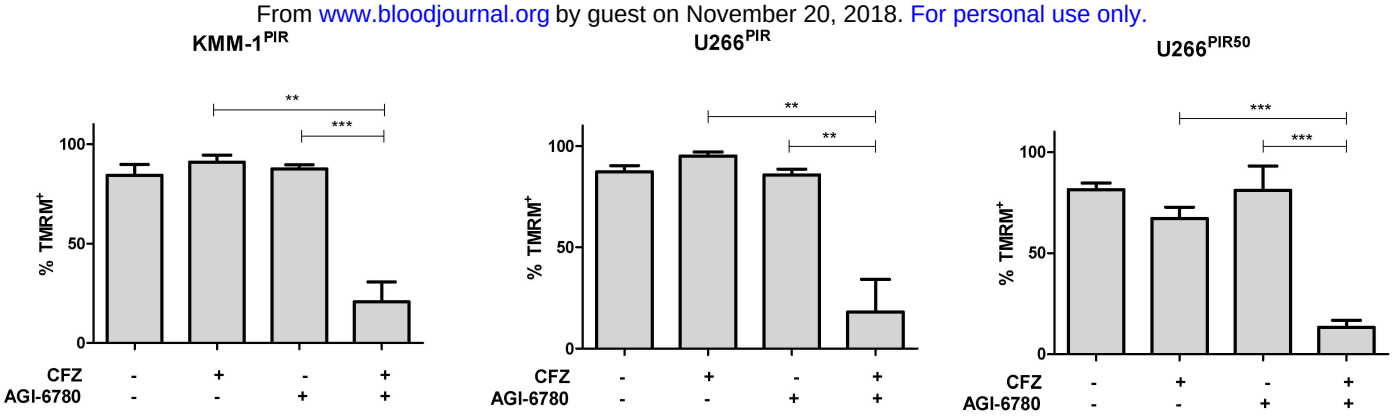

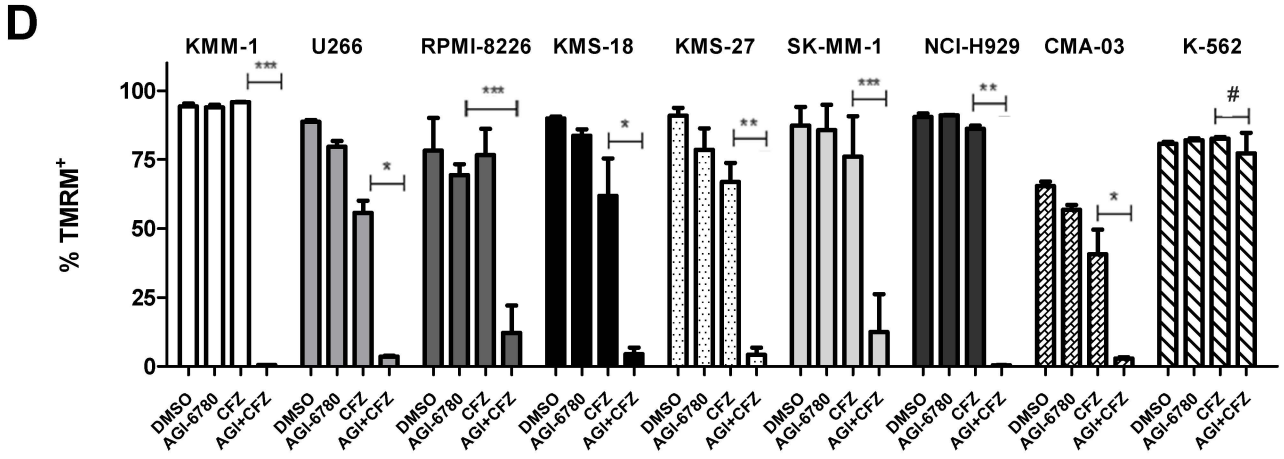

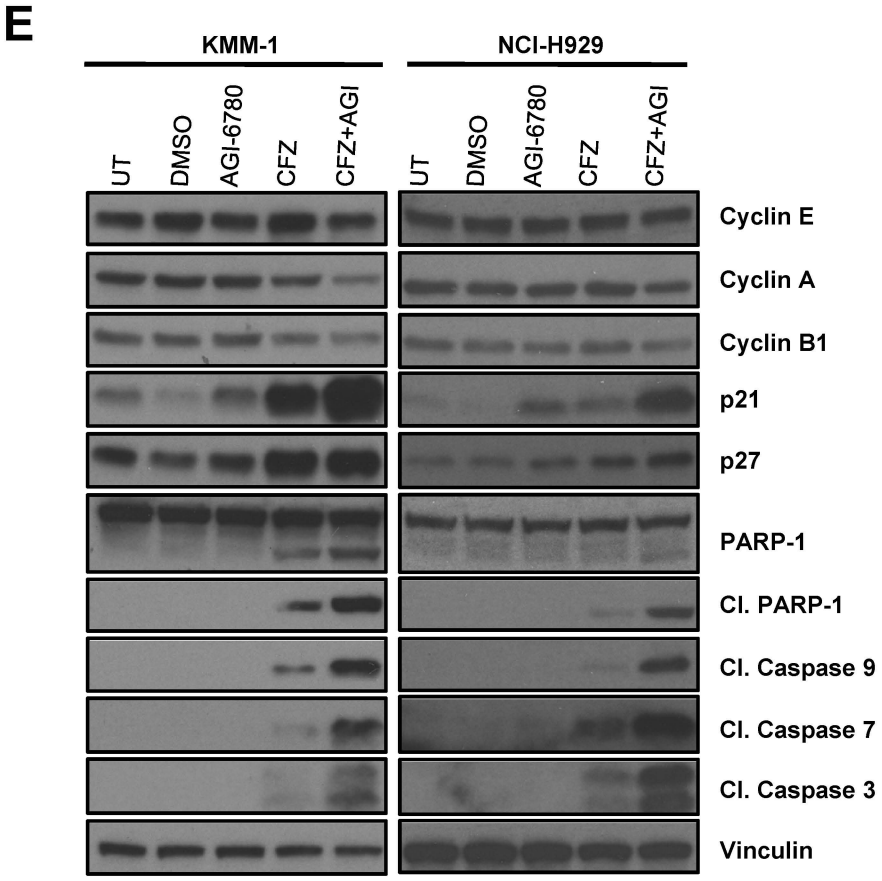

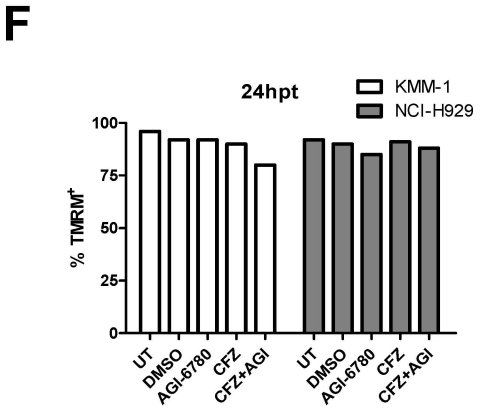

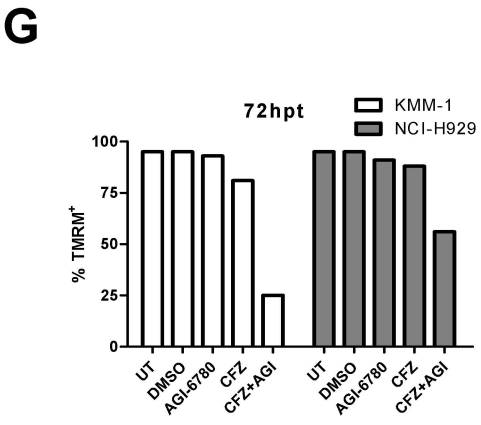

Fig. 2

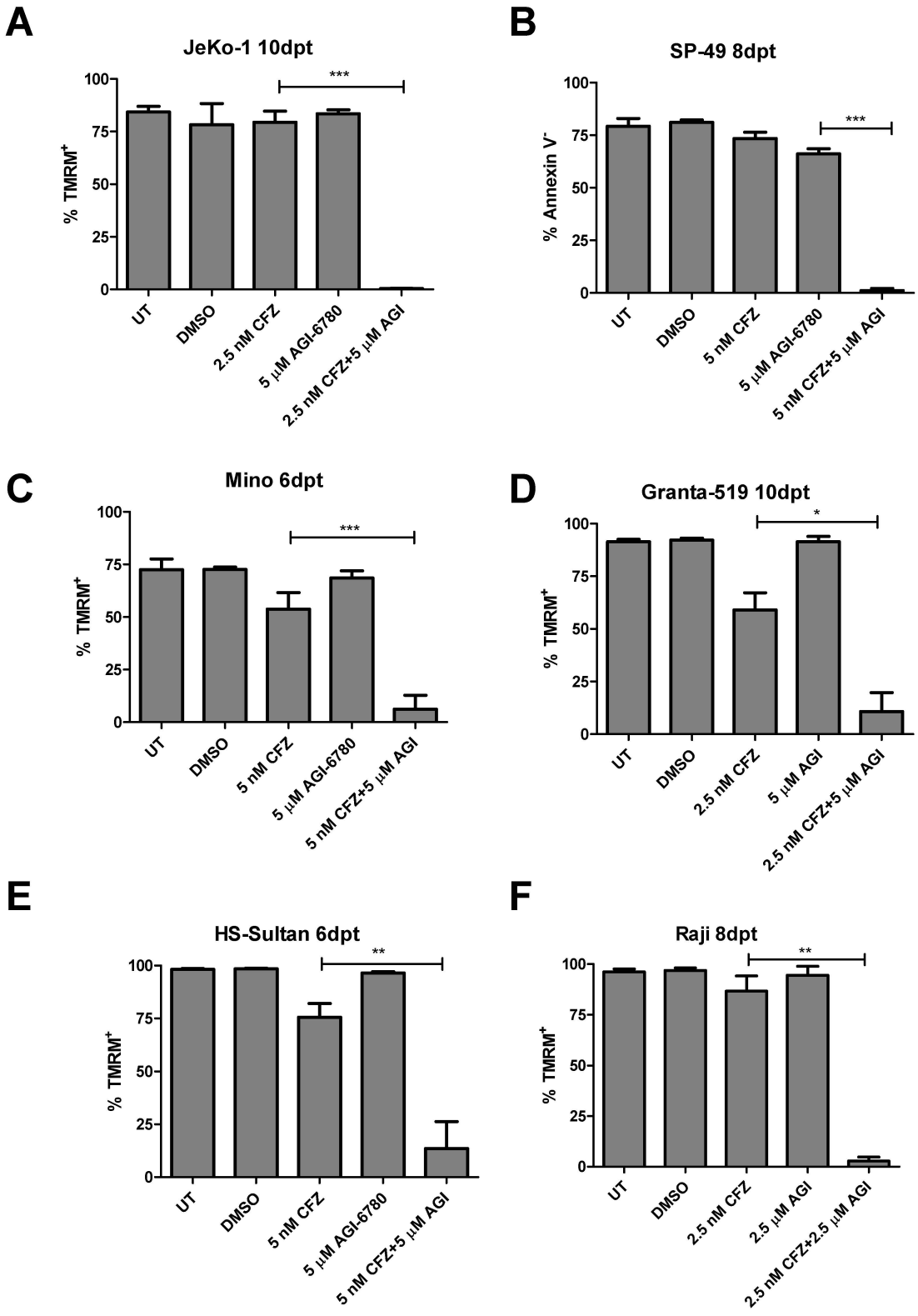

Fig. 3

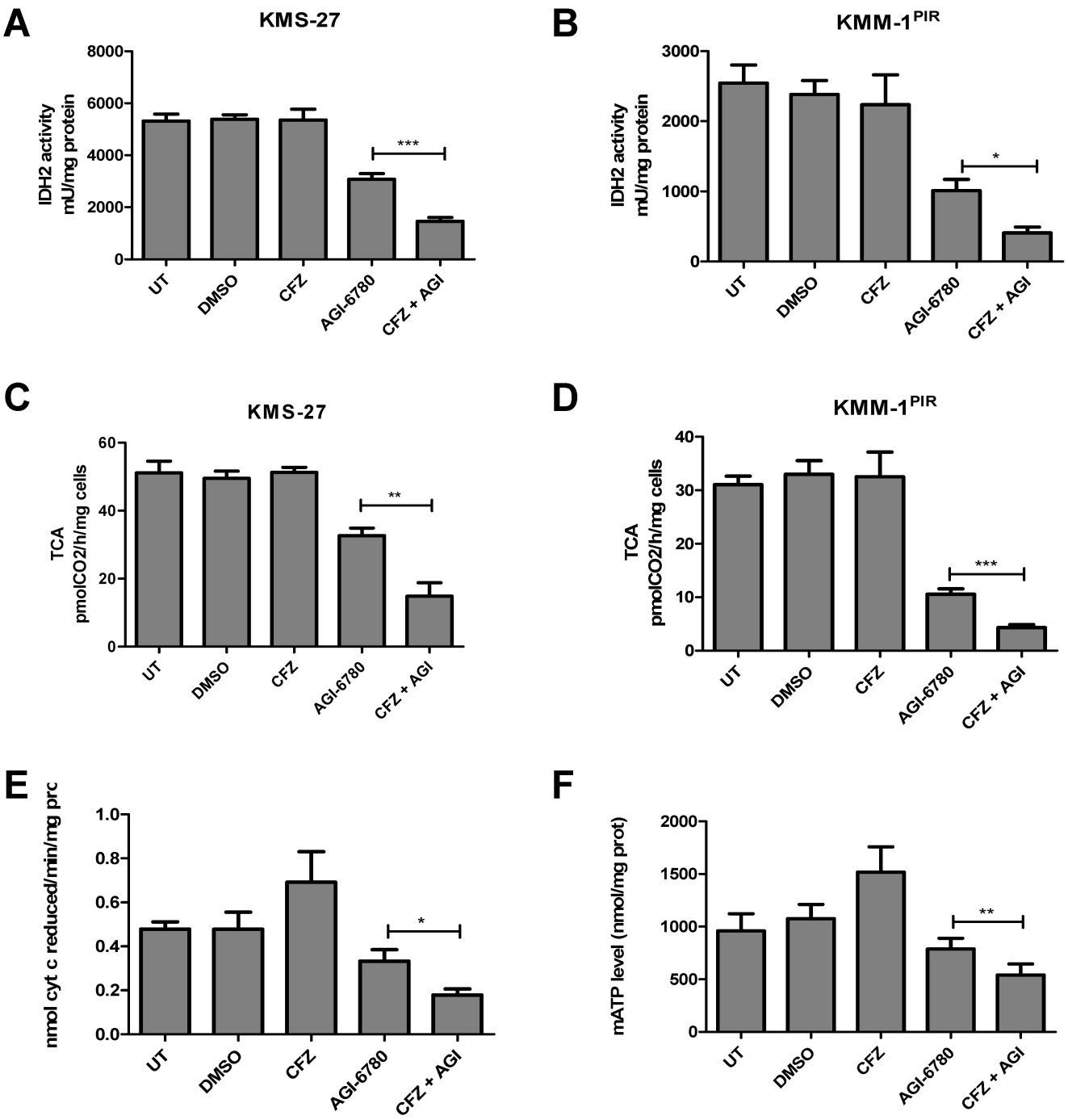

Fig. 4

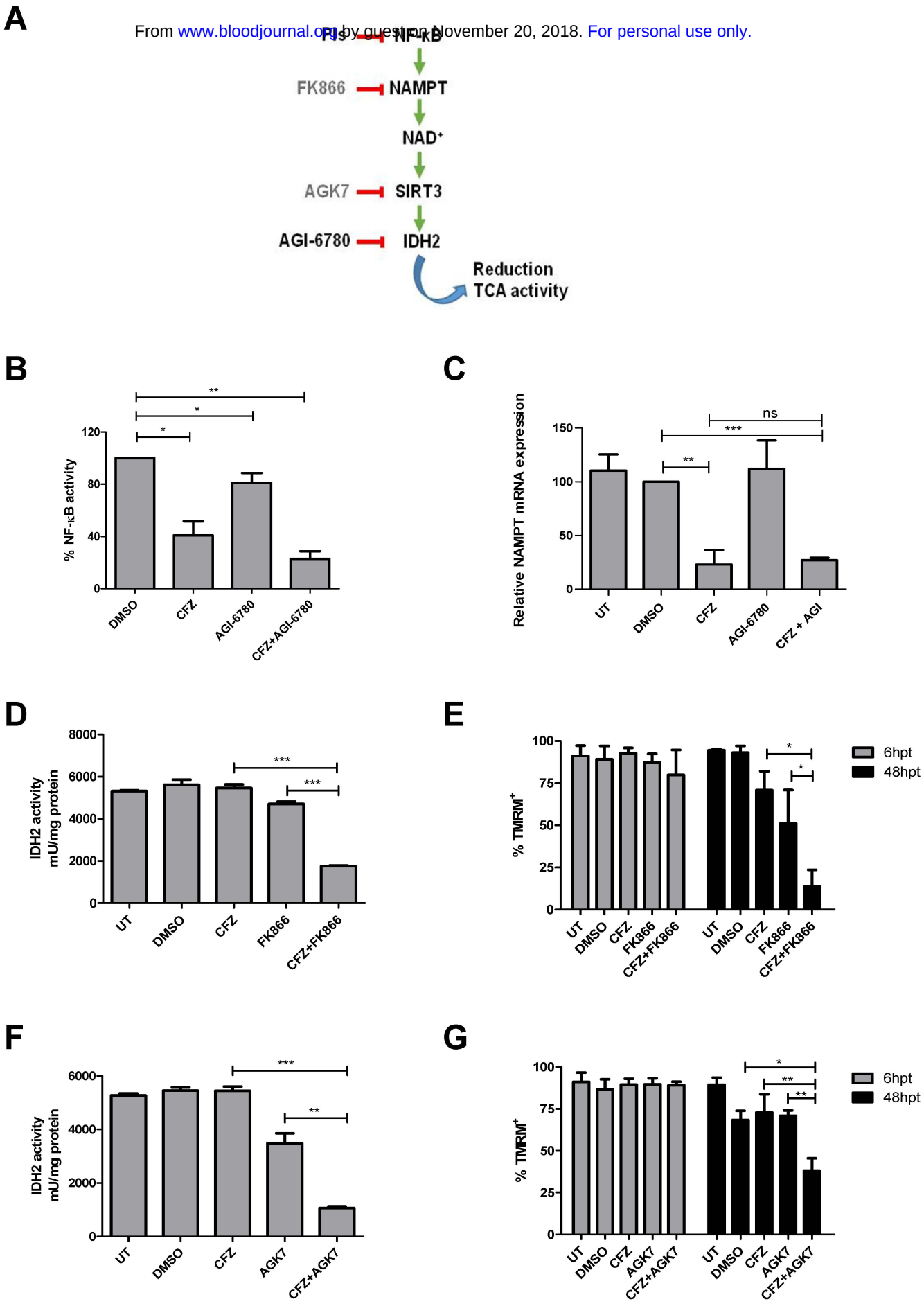

Fig. 5

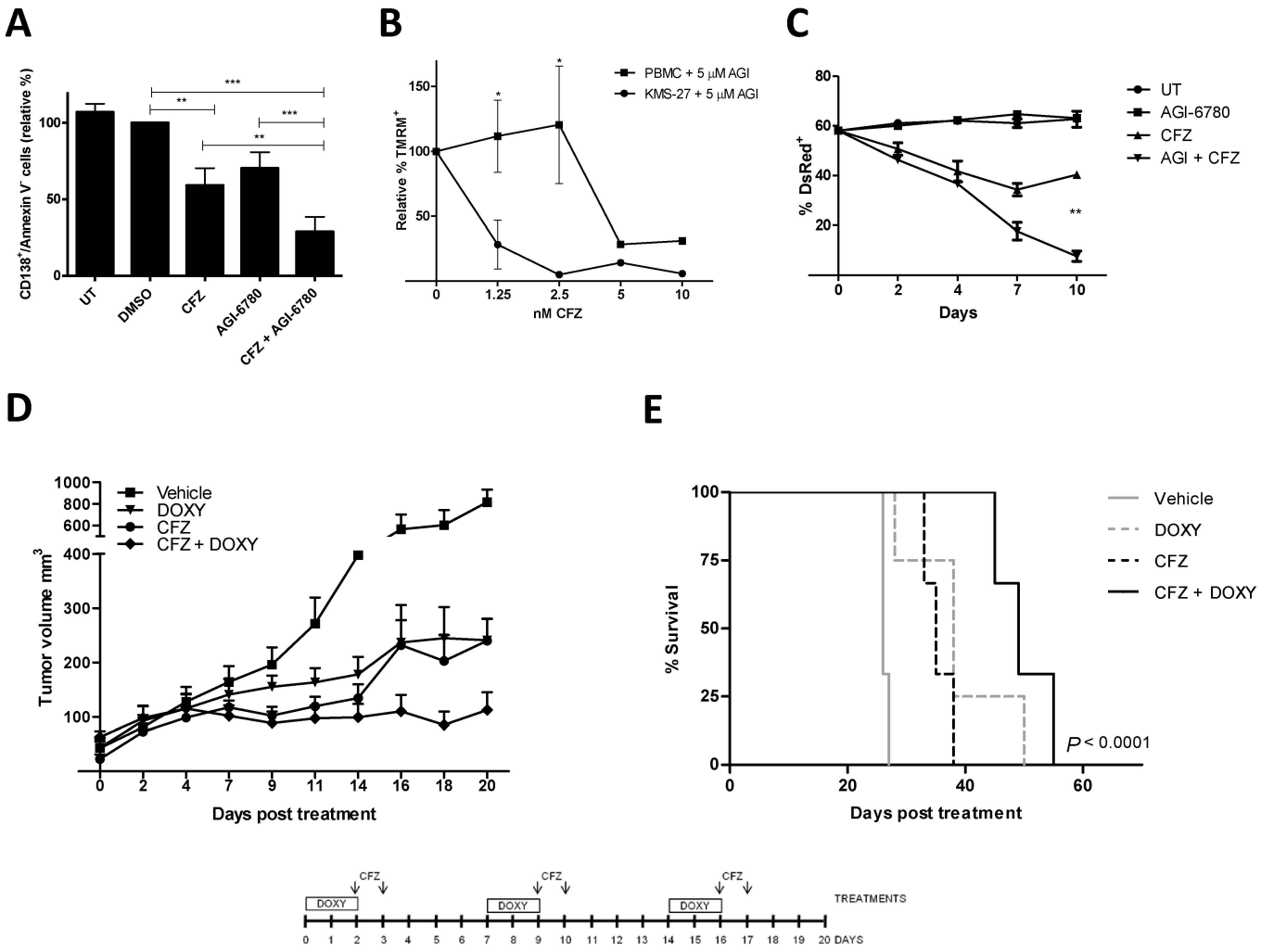

Fig. 6

Prepublished online November 19, 2018;
doi:10.1182/blood-2018-05-850826

IDH2 inhibition enhances proteasome inhibitor responsiveness in hematological malignancies

Elisa Bergaggio, Chiara Riganti, Giulia Garaffo, Nicoletta Vitale, Elisabetta Mereu, Cecilia Bandini, Elisa Pellegrino, Verdiana Pullano, Paola Omedè, Katia Todoerti, Luciano Cascione, Valentina Audrito, Anna Riccio, Antonio Rossi, Francesco Bertoni, Silvia Deaglio, Antonino Neri, Antonio Palumbo and Roberto Piva

Blood (print ISSN 0006-4971, online ISSN 1528-0020), is published weekly by the American Society of Hematology, 2021 L St, NW, Suite 900, Washington DC 20036.